Scientific
Research
Publishing

Methanol Steam Reforming over Na-Doped ZnO-Al$_2$O$_3$ Catalysts

Di Liu, Yong Men*, Jinguo Wang, Xin Liu, Qiuyan Sun

College of Chemistry and Chemical Engineering, Shanghai University of Engineering Science, Shanghai, China
Email: *men@sues.edu.cn

Abstract

In this study, the catalyst composition in binary ZnO-Al$_2$O$_3$ catalyst was initially evaluated and optimized for methanol steam reforming. Then different Na contents were loaded by an incipient wetness impregnation method onto the optimized ZnAl catalyst. It was found that the activity was greatly enhanced by the modification of Na, which depended on the Na content in the catalyst. The methanol conversion was 96% on a 0.1 Na/0.4 ZnAl catalyst (GHSV = 14,040 h^{-1}, S/C = 1.4, 350°C), which was much higher with respect to a Na-free 0.4 ZnAl catalyst (74%). The remarkable improvement of activity was attributed to a weakening of the C-H bonds and clear of hydroxyl group by the Na dopant leading to an accelerated dehydrogenation of the reaction intermediates formed on ZnAl$_2$O$_4$ spinel surface and thus the overall reaction.
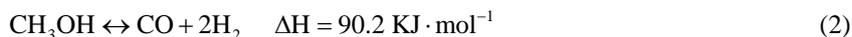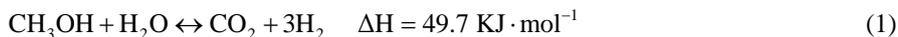
Keywords

1. Introduction

As electronic devices become smaller and more complex, hydrogen-fed compact fuel cell systems become a feasible solution for the resulting power requirements, replacing current Li-ion batteries. The on-board storage of pressurized hydrogen is inherently problematic for a mobile device because of an increased balance of plant resulting in a lowered overall power density of the device [1]. Methanol is considered as an ideal choice for on-demand production of hydrogen because of its high H/C ratio, low boiling point and no C-C bond [2]-[4]. Under ideal conditions, the reaction can convert methanol and water into carbon dioxide and three moles of hydrogen in a moderately endothermic transformation, as shown in Equation (1). However, there are always with other side reactions, methanol decomposition Equation (2) and water-gas shift reaction Equation (3)

---

*Corresponding author.

[5]-[7].

$$CH_3OH + H_2O \leftrightarrow CO_2 + 3H_2 \quad \Delta H = 49.7 \text{ KJ} \cdot \text{mol}^{-1} \tag{1}$$

$$CH_3OH \leftrightarrow CO + 2H_2 \quad \Delta H = 90.2 \text{ KJ} \cdot \text{mol}^{-1} \tag{2}$$

$$CO + H_2O \leftrightarrow CO_2 + H_2 \quad \Delta H = -41.2 \text{ KJ} \cdot \text{mol}^{-1} \tag{3}$$

Recent years, much research has been focused on the Cu-based catalysts especially Cu/ZnO and Cu/ZnO/Al$_2$O$_3$ owing to their low cost and relatively high catalytic activity. However, Cu-based catalysts are pyrophoric and easily deactivated at elevated temperature, which goes against to the application in fuel cell [8]-[11]. It is very attractive to develop a green, inexpensive and efficient high-temperature steam reforming catalyst with low CO concentration and long-term stability. Yang *et al.* [12] reported that ZnO-Al$_2$O$_3$ exhibited high activity and generated hydrogen-rich reformate with low CO concentration for high-temperature steam reforming of methanol.

Since highly efficient-catalyst systems are always desirable, new approaches of catalyst promotion are necessary. Recent literatures [13] [14] demonstrated that alkali-promoted Pt-based catalysts exhibited high activities in various reactions such as preferential CO oxidation (PROX), water-gas shift reaction and low-temperature oxidation of formaldehyde [15] [16]. In water-gas shift reaction, alkali-stabilized Pt-OH$_x$ species in Na- or K-promoted Pt/Al$_2$O$_3$ and Pt/SiO$_2$ catalysts were proposed to explain the reaction at low temperature, and the reaction pathway was dependent on the addition of alkali ions, as evidenced in HCHO oxidation over alkali metal-promoted Pt/TiO$_2$ and Pt/SiO$_2$ catalysts [17]. However, scant researches have been conducted on the Na-doped ZnO-Al$_2$O$_3$ catalysts for methanol steam reforming reaction (MSR).

Herein, ZnO-Al$_2$O$_3$ and alkali-doped ZnO-Al$_2$O$_3$ catalysts were prepared by coprecipitation method and incipient-wetness impregnation method, respectively, and characterized by means of XRD, BET and FTIR. Many parameters including Zn/Al molar ratio, different Na loading were investigated and correlated with their catalytic properties. Reforming tests were performed under practical application conditions, *i.e.* without pretreatment or pre-reduction of the catalysts before testing.

2. Experimental Section

2.1. Catalyst Preparation

ZnO-Al$_2$O$_3$ catalyst was prepared by a co-precipitation method at a constant pH of 7 - 8. The Zn(NO$_3$)$_2$·6H$_2$O and Al(NO$_3$)$_3$·9H$_2$O were dissolved into 200 ml deionized water. The aqueous solution of metal nitrates with a total cation concentration of 1.0 M was contacted with a basic solution of aqueous ammonium with a stoichiometric molar ratio. The process was carried out by dropwise addition of both solutions into a stirred flask containing 200 ml of de-ionized water at room temperature. The precipitate formed was aged in the mother liquid for 1 h, then removed, washed with de-ionized water several times and centrifuged. The obtained deposit was dried at 90°C for 8 h and calcined at 500°C for 3 h. The catalyst was then ground, pressed, crushed and screened to 40 - 60 mesh. The resultant ZnO-Al$_2$O$_3$ samples are designated as X ZnAl, in which the symbol X represents the ZnO/(ZnO + Al$_2$O$_3$) molar ratio.

The Na-doped ZnO-Al$_2$O$_3$ catalysts were prepared by incipient-wetness impregnation method, the precursor solution was sodium acetate, and the optimized catalyst (0.4 ZnAl) was then taken as the support in this study. After sodium metal precursor solution with different mass loadings (0.1 wt% - 3 wt%) were impregnated on support, then followed by standing at room temperature for 12 h, and then dried at 110°C for 12 h, finally calcined at 500°C for 4 h in air. The resultant Na-doped ZnO-Al$_2$O$_3$ samples are designated as ZNa/0.4 ZnAl, in which the Z represents the content of sodium metal (wt%).

2.2. Catalyst Characterizations

X-ray diffraction (XRD) measurements were carried out on a BRUKER D2 PHASER with Cu Kα radiation (λ = 0.15406 nm, 30 kV/10 mA). N$_2$ adsorption-desorption isotherms were recorded on a Micromeritics ASAP 2460 instrument at 77 K, from which the surface area (S_{BET}), pore volume (V_P) and pore diameter (D_P) were calculated by applying the Brunauer-Emmett-Teller (BET) and Barrett-Joyner-Halenda (BJH) models to the desorption branches. Fourier-transform infrared (FT-IR) spectra at room temperature were recorded on a Nicolet 380 spectrometer (USA) infrared spectrometer.

2.3. Catalytic Activity Measurements

The MSR reaction was carried out in a flowing-type quartz tube fixed bed reactor containing 200 mg of 40 - 60 mesh catalysts under atmospheric pressure from 200°C to 500°C, which was controlled by a thermocouple placed in the center of the catalyst bed. The mixture containing H_2O and CH_3OH in a liquid tank with the desired H_2O/CH_3OH mole ratio was injected continuously to a vaporizer at 200°C by a syringe pump at a rate of 1.2 $cm^3 \cdot h^{-1}$ to vaporize methanol and water, and then carried into the catalytic reactor by N_2 with GHSV at 14,040 h^{-1}.

The product effluents from the reactor were analyzed quantitatively by an on-line gas chromatograph (GC-2014C, Shimadzu) equipped with thermal conductivity detector (TCD) and flame ionization detector (FID). The methanol conversion, product selectivity, and gas-hourly space velocity (GHSV) was calculated by using Equations (4)-(6), respectively:

$$\text{Methanol conversion } (\%) = \frac{C_{in(CH_3OH)} - C_{out(CH_3OH)}}{C_{in(CH_3OH)}} \times 100 \tag{4}$$

where $C_{in(CH_3OH)}$ and $C_{out(CH_3OH)}$ are the inlet and outlet methanol molar flows, respectively.

$$S_i (\%) = \frac{n_i C_i}{\sum \text{all product species } n_j C_j} \times 100 \tag{5}$$

where n_i is the molar flow rate of products (mol·min^{-1}); c_i is the number of carbon atoms or hydrogen atoms in every product's molecule. All the calculated selectivities were based on carbon atoms except H_2 based on hydrogen atoms.

$$\text{GHSV} = \frac{V_{CH_3OH} + V_{N_2} + V_{H_2O}}{V_{cat}} \times 60 \tag{6}$$

where V_{CH_3OH}, V_{N_2} and V_{H_2O} is the gaseous flow rate of CH_3OH, N_2 and H_2O in the feed (cm^3·min^{-1}) respectively, V_{cat} (cm^3) is the volume of catalysts.

3. Results and Discussion

3.1. Catalyst Characterizations

3.1.1. XRD

The XRD patterns in **Figure 1** show that all the catalysts displayed diffraction peaks at 2θ of 31.2°, 36.8°, 44.8°, 55.6°, 59.3° and 65.2° ($ZnAl_2O_4$ JCPDS Card No. 05-0669) suggesting that ZnO and Al_2O_3 easily formed the spinel structure after calcination at temperatures exceeding 500°C [12] [18]. No diffraction peaks of alkali metal species could be observed owing to the low alkali metal loading or its presence in form of highly dispersed nanoparticles on the catalyst surface. It was also suggested that Na doping could not affect the original crystal structure of the catalyst.

3.1.2. BET

Based on N_2 adsorption-desorption isotherms in **Figure 2**, the SBET, VP and DP could be calculated by using the BET and BJH models, respectively. All the catalysts displayed the type-IV N_2 adsorption-desorption isotherms with H_2 hysteresis loops indicative of the typical mesoporous structure of the alumina support owing to the agglomeration of nanoparticles. The corresponding pore size distribution curves showed a relatively narrow pore diameter range centered at about 4 - 5 nm. As shown in **Table 1**, the surface area of catalysts decreased gradually with doping Na content while the average pore diameter almost kept unchanged, indicating that Na homogeneously dispersed on the external surface of 0.4 ZnAl and part of the Na blocked the pore structure of the 0.4 ZnAl.

3.1.3. FTIR

In order to further understand the catalytic behaviors of the catalysts, FTIR experiments were conducted on the 0.4 ZnAl and 0.1 Na/0.4 ZnAl catalysts, and the results are shown in **Figure 3**. As demonstrated in the literature [19] by diffuse reflectance infrared Fourier transform (DRIFT) investigations, the main reason for these enhanced activities is a weakening of the C-H bonds of the formate intermediates by the alkali dopant leading to an accelerated dehydrogenation of the reaction intermediates. Starting with the spectra of the 0.4 ZnAl, the C-H
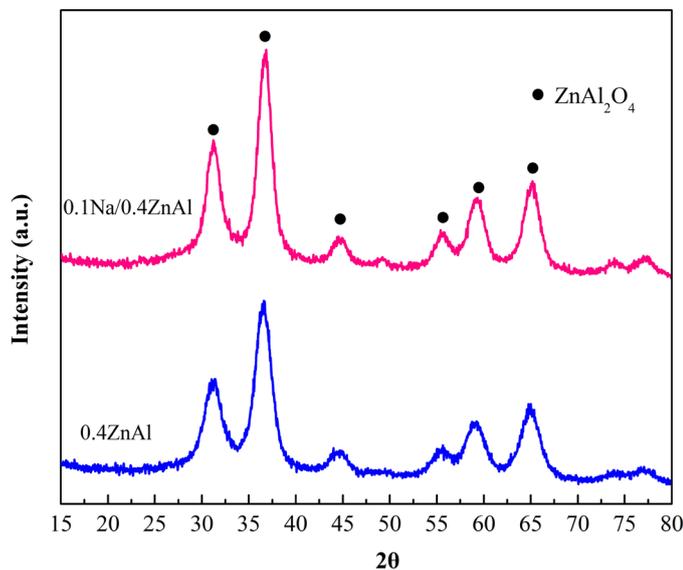
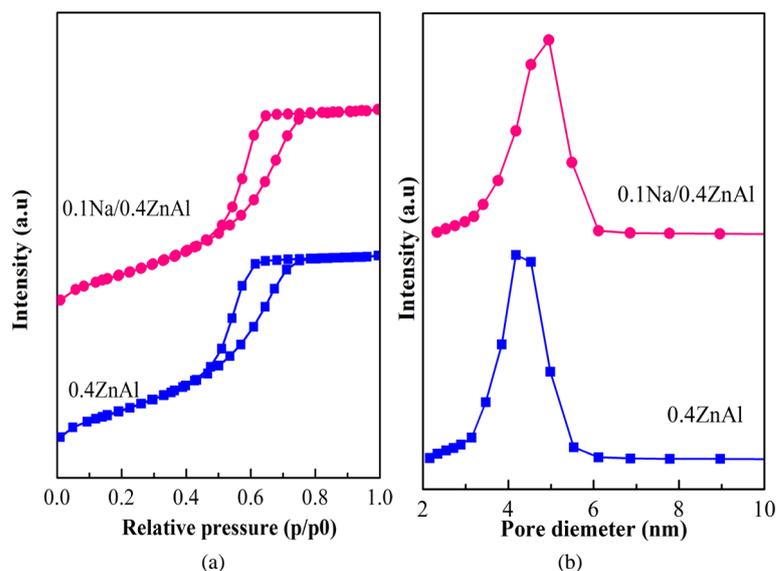**Figure 1.** XRD patterns of 0.4 ZnAl and 0.1 Na/0.4 ZnAl catalysts.

Figure 2. N_2 adsorption-desorption isotherms (a) and pore size distribution curves (b) of 0.4 ZnAl and 0.1 Na/0.4 ZnAl catalysts.

Table 1. Physical structural parameters of different catalysts.

Catalyst	S_{BET} (m²/g)	D_p (nm)	V_p (cm³/g)
0.4 ZnAl	133.0	4.2	0.189
0.1 Na/0.4 ZnAl	125.4	4.6	0.195

bonds of the methyl is visible at 1460 cm⁻¹ and a more intense feature at 3670 cm⁻¹ is O-H bonds. The intensity of the band at 1460 cm⁻¹ had a little weaken of Na-doped 0.4 ZnAl catalysts, this was consistent with the literatures which resulted enhanced activity. And apparently, the peak of the O-H bands at 3670 cm⁻¹ became sharper for 0.1 Na/0.4 ZnAl catalyst. That indicated the free hydroxyl group became more evident on the surface of 0.1 Na/0.4 ZnAl catalyst, which rendered methanol easier to catch hydroxyl group to participate in the reaction and improve the conversion.
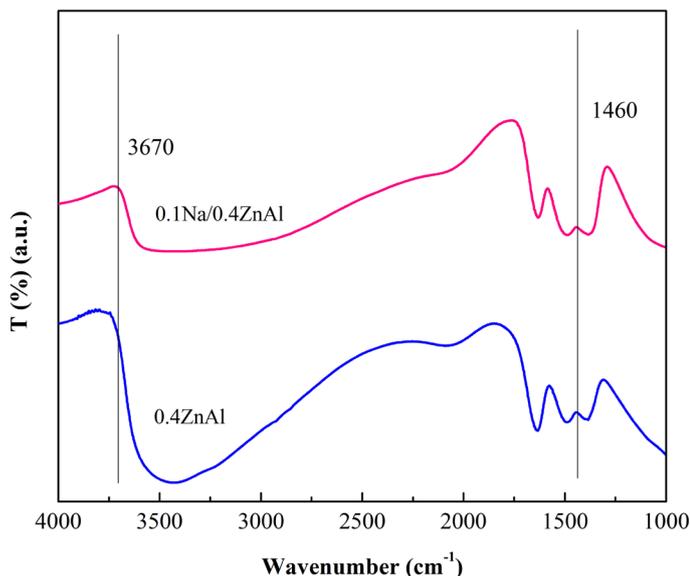
Figure 3. FTIR spectra of 0.4 ZnAl and 0.1 Na/0.4 ZnAl catalysts.

3.2. Catalytic Performances

3.2.1. Zn:Al Molar Ratio

Figure 4 shows the effect of different Zn:Al molar ratio in the catalyst on methanol conversion and product selectivity over different catalysts. For all these catalysts, the methanol conversion increased with increasing reaction temperature. Among them, 0.4 ZnAl catalyst had the highest methanol conversion, approaching the complete conversion at 390˚C. However, the methanol conversion declined when the Zn:Al molar ratio exceeded 0.4. For 0.24 ZnAl catalyst, it was giving a rather low activity and the full conversion after 430˚C. The catalyst without Zn showed the worst activity, not able to get a reasonable conversion even at high reaction temperature of 500˚C. From the **Figure 4(b)**, it was obvious that Zn:Al molar ratio also had a significant effect on products selectivity. The dimethyl ether selectivity reached nearly 100% of Al_2O_3 catalyst, which indicated Al_2O_3 has strong acid sites. When the molar ratio of Zn increased to 0.24, the selectivity of dimethyl ether had an apparent decrease from 99% to 20% and disappeared on 0.4 ZnAl and 0.5 ZnAl catalysts. It was clear that 0.4 ZnAl catalyst had the highest conversion and H_2 selectivity and CO selectivity was as low as 2% at 390˚C. As a result, the optimal Zn:Al molar ratio was determined to 0.4.

3.2.2. The Effect of Na Content

Figure 5 showed the effect of Na content in 0.4 ZnAl catalysts on methanol conversion and product selectivity at 350˚C. The results illustrates that the Na loading has little effect on products selectivity. However, the catalysts activity was significantly improved by Na addition. Na-doped 0.4 ZnAl catalysts had the best activity in only 0.1 wt% doping amount. When the Na content exceed 0.1 wt%, the activity dropped at 0.3 wt% and then increased again at 1 wt%.

It is obvious that Na-doped can perform the best to promote the activity, as that the methanol conversion increased from 74% to 96% of 0.1 Na/0.4 ZnAl. The activity data of Na-doped 0.4 ZnAl catalysts is consistent with the results in **Figure 3**, implying that the more clearly the hydroxyl group on the surface and more weaken of C-H bonds of catalysts, the higher of reforming activity. The weaken effect of C-H bond resulted in the easier dehydrogenation of methanol to form formaldehyde, which was the key intermediate of methanol reforming reacting with hydroxyl group to form the desired CO_2 and H_2.

4. Conclusion

In summary, a series of Na-doped 0.4 ZnAl catalysts prepared by the incipient-wetness impregnation method were tested under conditions of methanol steam reforming (MSR) with the temperature range from 200˚C to 500˚C. The loading of Na on 0.4 ZnAl in this study varied from 0.1 wt% to 3 wt%. Many effective parameters
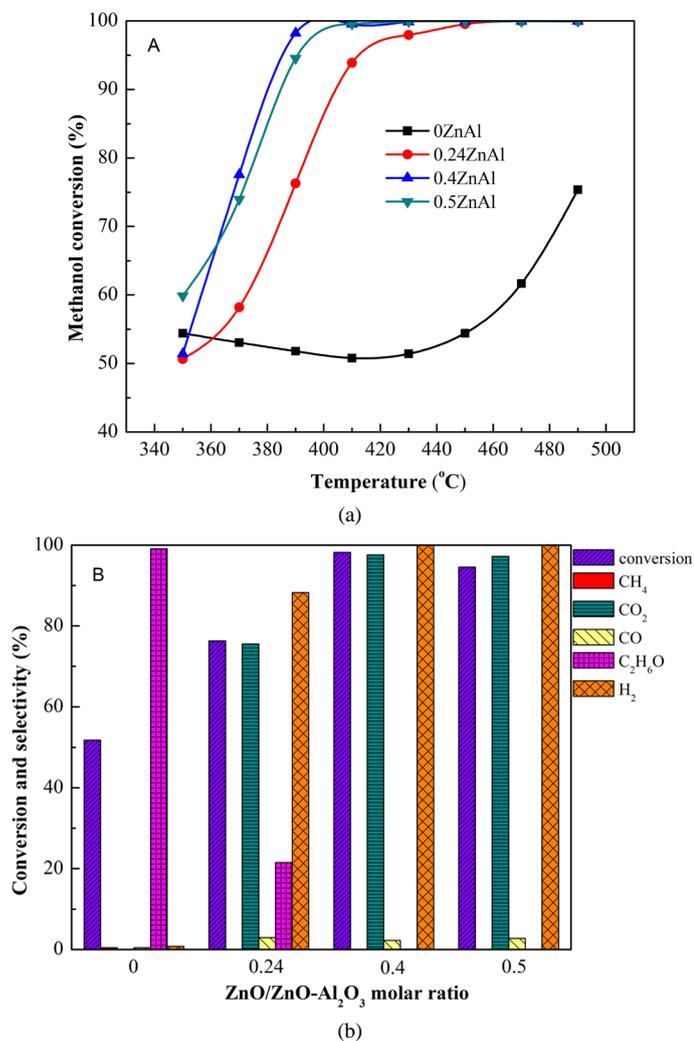
(a)

(b)

Figure 4. Effect of Zn:Al molar ratio on methanol conversion (a) and product selectivity (b); of different catalysts at 390°C. Condition: liquid feed rate = 1.2 cm^3·h^{-1}, S/C = 1.4, N$_2$ flow rate = 30 cm^3·min^{-1}, amount of catalyst = 0.20 g, 1 bar.
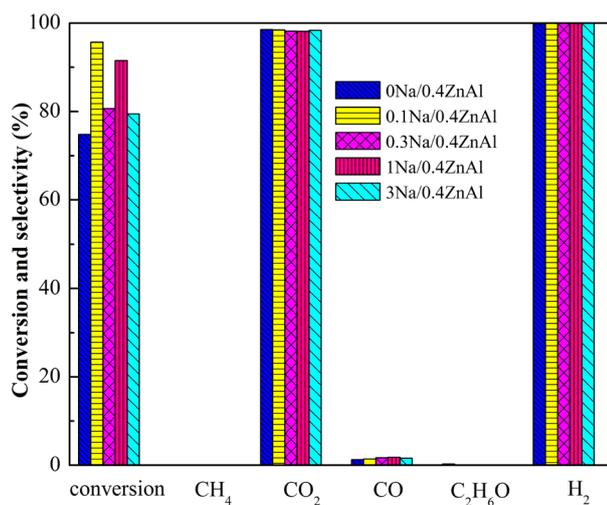

Figure 5. Effect of Na loading in 0.4 ZnAl catalysts on methanol conversion and product selectivity at 350°C. Condition: liquid feed rate = 1.2 cm^3·h^{-1}, S/C = 1.4, N$_2$ flow rate = 30 cm^3·min^{-1}, amount of catalyst = 0.20 g, 1 bar.

such as reaction temperature, ZnAl molar ratio, and Na loading were also investigated and the corresponding optimal parameters were 350˚C, 0.4, 0.1 wt%, and Na, respectively. As a result, the 0.1 Na/0.4 ZnAl catalyst exhibited the highest methanol conversion (96%), very high H_2 selectivity (99.9%) and low CO selectivity (1.4%) at the optimal conditions. The improvement of activity is mainly caused by the weakening effect of C-H bond and more populated hydroxyl group on catalysts surface. The results suggested that 0.1 Na/0.4 ZnAl might serve as a promising catalyst for the hydrogen production via methanol steam reforming for fuel cell applications.

Acknowledgements

References

[1] Conant, T., Karim, A., Lebarbier, V., Wang, Y., Girgsdies, F., Schlogl, R., *et al*. (2008) Stability of Bimetallic Pd-Zn Catalysts for the Steam Reforming of Methanol. *Journal of Catalysis*, **257**, 64-70. http://dx.doi.org/10.1016/j.jcat.2008.04.018

[2] Sá, S., Silva, H., Brandão, L., Sousa, J.M. and Mendes, A. (2010) Catalysts for Methanol Steam Reforming—A Review. *Applied Catalysis B*: *Environmental*, **99**, 43-57. http://dx.doi.org/10.1016/j.apcatb.2010.06.015

[3] Yi, N., Si, R., Saltsburg, H. and Flytzani-Stephanopoulos, M. (2010) Steam Reforming of Methanol over Ceria and Gold-Ceria Nanoshapes. *Applied Catalysis B*: *Environmental*, **95**, 87-92. http://dx.doi.org/10.1016/j.apcatb.2009.12.012

[4] Palo, D.R., Dagle, R.A. and Holladay, J.D. (2007) Methanol Steam Reforming for Hydrogen Production. *Chemical Reviews*, **107**, 3992-4021. http://dx.doi.org/10.1021/cr050198b

[5] Lindstrom, B. and Pettersson, L.J. (2001) Hydrogen Generation by Steam Reforming of Methanol over Copper-Based Catalysts for Fuel Cell Applications. *International Journal of Hydrogen Energy*, 923-933. http://dx.doi.org/10.1016/S0360-3199(01)00034-9

[6] Brant, A., Peppley, J.C.A., Kearns, L.M. and Mann, R.F. (1999) Methanol-Steam Reforming on $Cu/ZnO/Al_2O_3$. Part 1: The Reaction Network. *Applied Catalysis A*: *General*, **179**, 21-29. http://dx.doi.org/10.1016/S0926-860X(98)00298-1

[7] Peppley, B.A., Amphlett, J.C., Kearns, L.M. and Mann, R.F. (1999) Methanol-Steam Reforming on $Cu/ZnO/Al_2O_3$ Catalysts. Part 2. A Comprehensive Kinetic Model. *Applied Catalysis A*: *General*, **179**, 31-49. http://dx.doi.org/10.1016/S0926-860X(98)00299-3

[8] Huang, C.Y., Sun, Y.M., Chou, C.Y. and Su, C.C. (2007) Performance of Catalysts $CuO-ZnO-Al_2O_3$, $CuO-ZnO-Al_2O_3$-Pt-Rh, and Pt-Rh in a Small Reformer for Hydrogen Generation. *Journal of Power Sources*, **166**, 450-457. http://dx.doi.org/10.1016/j.jpowsour.2006.12.045

[9] Kniep, B., Girgsdies, F. and Ressler, T. (2005) Effect of Precipitate Aging on the Microstructural Characteristics of Cu/ZnO Catalysts for Methanol Steam Reforming. *Journal of Catalysis*, **236**, 34-44. http://dx.doi.org/10.1016/j.jcat.2005.09.001

[10] Kniep, B.L., Ressler, T., Rabis, A., Girgsdies, F., Baenitz, M., Steglich, F., *et al*. (2004) Rational Design of Nanostructured Copper-Zinc Oxide Catalysts for the Steam Reforming of Methanol. *Angewandte Chemie International Edition in English*, **43**, 112-115. http://dx.doi.org/10.1002/anie.200352148

[11] Yongtaek Choi, H.G.S. (2002) Fuel Cell Grade Hydrogen from Methanol on a Commercial $Cu/ZnO/Al_2O_3$ Catalyst. *Applied Catalysis B*: *Environmental*, **38**, 259-269. http://dx.doi.org/10.1016/S0926-3373(02)00054-1

[12] Yang, M., Li, S. and Chen, G. (2011) High-Temperature Steam Reforming of Methanol over $ZnO-Al_2O_3$ Catalysts. *Applied Catalysis B*: *Environmental*, **101**, 409-416. http://dx.doi.org/10.1016/j.apcatb.2010.10.010

[13] Kuriyama, M., Tanaka, H., Ito, S., Kubota, T., Miyao, T., Naito, S., *et al*. (2007) Promoting Mechanism of Potassium in Preferential CO Oxidation on Pt/Al_2O_3. *Journal of Catalysis*, **252**, 39-48. http://dx.doi.org/10.1016/j.jcat.2007.09.001

[14] Minemura, Y., Kuriyama, M., Ito, S.-I., Tomishige, K. and Kunimori, K. (2006) Additive Effect of Alkali Metal Ions on Preferential CO Oxidation over Pt/Al_2O_3. *Catalysis Communications*, **7**, 623-626.

http://dx.doi.org/10.1016/j.catcom.2006.01.028

[15] Zhai, Y., Pierre, D., Si, R., Deng, W., Ferrin, P., Nilekar, A.U., *et al.* (2010) Alkali-Stabilized Pt-OHx Species Catalyze Low-Temperature Water-Gas Shift Reactions. *Science*, **329**, 1633-1636. http://dx.doi.org/10.1126/science.1192449

[16] Ming Yang, S.L., Wang, Y., Herron, J.A., Xu, Y., Allard, L.F., Lee, S., Huang, J., Mavrikakis, M. and Flytzani-Stephanopoulos, M. (2014) Catalytically Active Au-O(OH)$_x$ Species Stabilized by Alkali Ions on Zeolites and Mesoporous Oxides. *Science*, **346**, 1498-1501. http://dx.doi.org/10.1126/science.1260526

[17] Zhang, C., Liu, F., Zhai, Y., Ariga, H., Yi, N., Liu, Y., *et al.* (2012) Alkali-Metal-Promoted Pt/TiO$_2$ Opens a More Efficient Pathway to Formaldehyde Oxidation at Ambient Temperatures. *Angewandte Chemie International Edition in English*, **51**, 9628-9632. http://dx.doi.org/10.1002/anie.201202034

[18] Yang, M., Men, Y., Li, S. and Chen, G. (2012) Hydrogen Production by Steam Reforming of Dimethyl Ether over ZnO-Al$_2$O$_3$ Bi-Functional Catalyst. *International Journal of Hydrogen Energy*, **37**, 8360-8369. http://dx.doi.org/10.1016/j.ijhydene.2012.02.070

[19] Evin, H.N., Jacobs, G., Ruiz-Martinez, J., Graham, U.M., Dozier, A., Thomas, G., *et al.* (2007) Low Temperature Water-Gas Shift/Methanol Steam Reforming: Alkali Doping to Facilitate the Scission of Formate and Methoxy C-H Bonds over Pt/ceria Catalyst. *Catalysis Letters*, **122**, 9-19. http://dx.doi.org/10.1007/s10562-007-9352-x